Materials Research Proceedings 41 (2024) 1544-1550 https://doi.org/10.21741/9781644903131-171

# Formability analysis of incrementally hole-flanged parts using different tool sizes

BORREGO-PUCHE Marcos[1,a], PALOMO-VÁZQUEZ David[1,b], MORALES-PALMA Domingo[1,c], MARTÍNEZ-DONAIRE Andres Jesus[1,d *], CENTENO Gabriel[1,e], VALLELLANO Carpoforo[1,f]

[1]Department of Mechanical and Manufacturing Engineering, University of Sevilla, Spain

[a]mborrego@us.es, [b]dpalomo1@us.es, [c]dmpalma@us.es, [d]ajmd@us.es, [e]gaceba@us.es, [f]carpofor@us.es

**Keywords:** Sheet Metal Forming, SPIF, Flanging, Formability, Flangeability

**Abstract.** This contribution analyses the formability of incrementally hole flanged parts using different tool radii (10, 20 and 47.9 mm). The smallest radius (10 mm) can induce full incremental benefits in the hole-flanged specimen, whereas the biggest one generates a formability behaviour closer to a conventional press forming. In the first case, the necking process is clearly delayed, being the development of a fracture in the middle of the wall flange the mechanism that controls the failure of the specimen. In contrast, in the second case, failure is governed by the appearance and development of a neck at the edge of the flange, which ends in material fracture. The intermediate tool radius (20 mm) shows midway features between a conventional and a fully incrementally formed specimen. The location and fracture mode of the flanged parts with different tool sizes are experimentally analysed and discussed within the Forming Limit Diagram (FLD) using the optical strain measurement system ARGUS®.

## Introduction

Hole flanges are commonly used in industry to provide stiffness or support for joining to other metallic parts. Usually performed by conventional press forming, it requires robust machinery and dedicated setups. For this reason, only a great number of operations justify the investment in this forming process. In recent decades, the use of incremental forming processes has been extended, particularly its simplest version, known as Single Point Incremental Forming (SPIF). This relative new forming process, whose first patents date back to 1967, not only addresses the disadvantages mentioned above, answering the increasing demand of flexible and cost-effective tooling, but also has a great advantage over conventional forming processes from the formability point of view. In this sense, the paper by Emmens and van den Boogaard [1] collects the most significant contributions that have been proposed to explain plastic deformation of incremental forming processes above the Forming Limit Curve (FLC) at necking. Among them, Silva et al. [2] proposed fracture as the key failure mechanism and, therefore, that localised necking typical of conventional sheet metal forming is inhibited in SPIF. Lately, new explanations for the increase of the FLC above the one obtained by conventional Nakazima tests have been suggested. Silva et al. [3] pointed out that it could be due to the stabilising effect of dynamic bending under tension. Authors carried out experimental work on AA1050-H111 with a series of truncated pyramidal and conical shapes under SPIF conditions for a range of tool sizes from 4 to 25 mm radius. Martínez-Donaire et al. [4] analysed the role of the level of average stress triaxiality attained in incremental processes, in the light of experimental and numerical results in hole flanging operations by single-stage SPIF on AA7075-O sheets.

In addition to the number of authors studying this phenomenon from the forces / stress point of view, many other authors maintain that the reason for the improvement in formability lies in the

microstructure [5-6]. Mosecker et al. [5] analysed the microstructural evolution with the increase in plastic strain under different parameters for Ti6Al4V sheet incremental forming of Ti6Al4V sheets. More recently, Chang et al. [6] characterised grain fragmentation, orientation, void deformation, and deformation dislocation by EBSD X-ray, SEM and TEM, concerning the incremental deformation of different regions around the contact area in truncated cone parts of AA5052-H32.

This paper presents an experimental investigation focused on analysing formability limits and failure mechanism in hole flanging by single-stage SPIF with hemispherical forming tools of increasing size (radii of 10, 20 and 47.9 mm) up to the target hole size (47.9 mm), where this limit situation corresponds in fact to a conventional press forming process. Results are analysed in terms of Limiting Forming Ratio (LFR) and fractographies of tested specimens to accurately assess the failure mechanism and strain distributions in the FLD.

**Experimental procedure**

A series of experimental hole flanging tests by single-stage SPIF with different pre-cut holes (*do*) and the same predefined target geometry were carried out on AA7075-O sheets of 1.6 mm thickness using hemispherical tools of different radii. The conventional press forming test corresponds to a limiting case of SPIF when the tool diameter and the final flange hole diameter match.

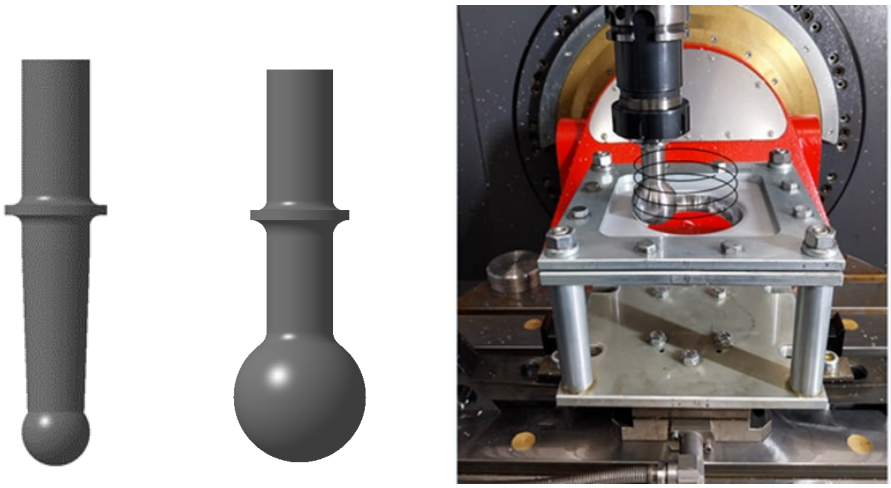

*Fig. 1. Schema of hemispherical tools and setup used in the hole flanging experiments by SPIF.*

The backing plate radius was 50 mm. All tests were carried out to obtain flanges with an inner radius of 47.9 mm considering the backing plate radius, the sheet thickness and a sheet-to-die clearance of 0.5 mm. The selected tool radii were 10, 20 and 47.9 mm. Fig. 1 presents a schema of the 10 and 20 mm radius tools and the experimental setup for single-stage SPIF. Fig. 2 shows the Erichsen machine for conventional press forming along with a schematic of the conventional hole flanging operation using the 47.9 mm punch radius.

An Emco Umill 630 machine was the selected machine for hole flanging tests by SPIF. The tool trajectory was programmed with CATIA®, following a 0.2 mm pitch helix with a feed rate of 1000 mm/min. No spindle rotation was used. The sheet-tool contact was sufficiently lubricated during the tests. For conventional forming tests, the Erichsen machine was employed under the recommendation of the standard ISO 12004-2 in terms of punch speed and tribological conditions. It should be noted that the forces reached for the 47.9 mm radius punch, i.e., in conventional forming, were an order of magnitude greater than in SPIF, exceeding the maximum force in the Z direction allowed by the Emco CNC machine.

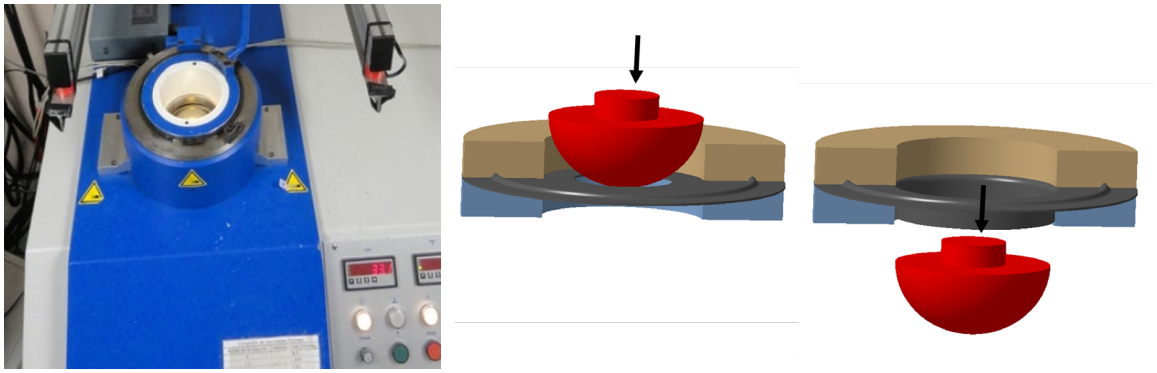

*Fig. 2. Erichsen machine setup and schema of conventional hole-flanging process.*

**Results and discussion**

This section presents and discusses the achieved Limiting Forming Ratio (*LFR*), fractographies of failed specimens, and strain analysis in the FLD.

Limiting Forming Ratio (*LFR*): In all tests where a failure-free flange was produced, the *HER* (Hole Expansion Ratio) was calculated as the $d_f/d_o$ ratio. Then, the measurement of formability was computed using the concept of *LFR* first introduced by Huang et al. [7,8], as the maximum *HER* attained by the material:

$$LFR \equiv HER_{max} \equiv \left.\frac{d_f}{d_o}\right|_{max} \quad (1)$$

where $d_f$ is the inner diameter of the produced hole-flanged part. A fixed value $d_f$ = 95.8 mm has been used.

Table 1 summarises the results of the experimental campaign carried out for different pre-cut holes and tool radii. Table 2 presents *LFR* values achieved for each tool radius. It is worth noting that the value of the *LFR* for 20 mm tool radius is the highest achieved, although this tool size is in between the other two tests.

*Table 1. Results of experimental hole flanging tests by single-stage SPIF and conventional press forming. 'X' stands for a failed flange and 'O' for a successful flange.*

| Hole flanging | Tool radius [mm] | Initial pre-cut hole diameter, $d_O$ [mm] | | | | | | | | | |
|---|---|---|---|---|---|---|---|---|---|---|---|
| | | 52 | 53 | 54 | 55 | 56 | 57 | 58 | 59 | 60 | 61 |
| SPIF | 10 | | | | X | X | X | O | | | |
| SPIF | 20 | X | | X | O | | | | | | |
| Press forming | 47.9 | | | | | | | X | | X | O |

*Table 2. LFR values in hole flanging by single-stage SPIF and conventional press forming.*

| Hole flanging | Tool radius [mm] | $d_{O,min}$ [mm] | *LFR* |
|---|---|---|---|
| SPIF | 10 | 58 | 1.65 |
| SPIF | 20 | 55 | 1.72 |
| Press forming | 47.9 | 61 | 1.57 |

Fractographies: The samples were carefully examined under the microscope and images of the failure were taken at x20 magnification to clearly see the failure mode. For the smallest tool radius (Fig. 3a), the failure occurred in the middle of the wall along the circumferential direction, while the others presented a failure at the flange edge. As expected, specimens tested by SPIF using the smallest tool radius presented fracture with a very incipient neck (i.e., almost inhibited necking), in contrast to specimens tested by conventional press forming, which showed fracture developed from previous necking (Fig. 3c). In the 20 mm radius tool test by SPIF, a fracture with previous necking was also observed (Fig. 3b).

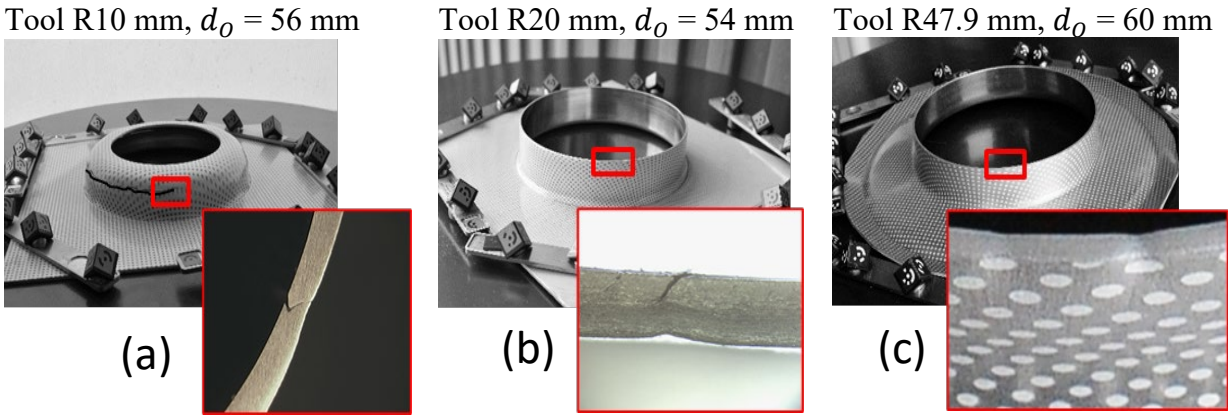


*Fig. 3. Failed tested specimens and fractographies with x20 magnification: (a) SPIF with 10 mm tool radius, (b) SPIF with 20 mm tool radius, and (c) conventional press forming.*

Strain analysis: Deformations were measured using the ARGUS® 3D optical system from a pattern of circular dots previously electroetched at the outer surface of the specimen. This system is unable to provide information near the free boundaries, that is, in fractured areas or at the edge of the hole. In such a case, the strains must be calculated from direct measurement of thickness and circumferential strains and assuming material volume constancy.

Fig. 4 depicts the evolution of the major and minor strain distributions measured on the outer surface of the specimens within the Forming Limit Diagram (FLD). The FLC (Forming Limit Curve at necking) and FFL (Fracture Forming Limit) for the material obtained in previous research [9] are also shown. The FLC was obtained following the time-dependent methodology proposed by Martínez-Donaire et al. [10] and the FFL was estimated by the procedure proposed by Cristino et al. [11]. Fig. 4 shows the contour map of the failed specimens. The location of the highest major strains, where the failure appeared, is indicated.

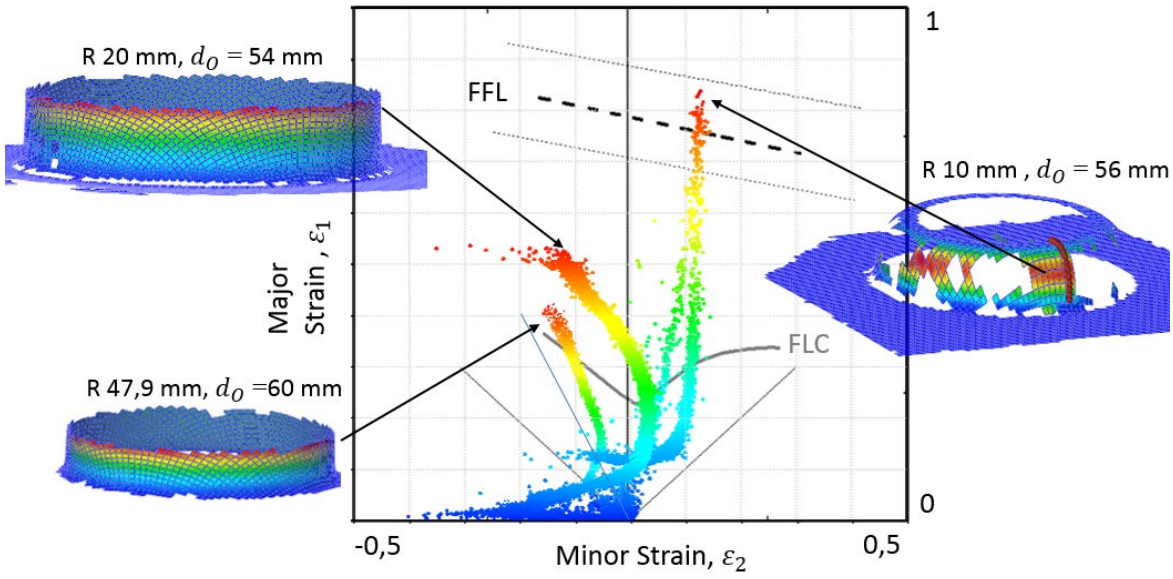


*Fig. 4. Major-minor strain distribution of the outer surface of failed specimens for 10 mm, 20 mm, and 47.9 mm tool radii in the Forming Limit Diagram of AA7075-O, 1.6 mm thickness.*

As mentioned above, the failure location was completely different despite the incremental nature of the process using 10 and 20 mm tool radii. A fracture was observed after a delayed or even suppressed necking in the middle of the wall using 10 mm tool radius. Instead, a fracture after a more severe necking at the flange edge occurred with the 20 mm tool radius, which is the same failure mechanism as in conventional flanging by press forming.

Regarding the location of the fracture using 20 mm tool radius, a priori it could be thought that the SPIF test using this tool is very similar to the conventional press forming process. Moreover, the shape of the strain distribution in both cases is very similar, as can be seen in the FLD depicted in Fig. 4. Both strain distributions present values close to plane strain stretching in the middle part of the flange wall, clearly between the uniaxial stretching and the biaxial stretching observed in the other tests.

However, there are clear differences between both processes. On the one hand, as can be seen in Fig. 4, the strains obtained by SPIF with a tool radius of 20 mm far exceed not only those obtained by conventional forming with a 47.9 mm punch radius, but also the FLC curve. This means that the conventional FLC is not applicable for SPIF even if the failure mechanism is necking. On the other hand, it should be noted that the strains of specimens tested by conventional forming slightly exceed the FLC (see Fig. 4) because of the bending induced in the material with respect to the Nakazima tests and the inherent experimental scatter, as discussed in previous research [12].

The hole flanging process by SPIF was proposed to address the drawbacks of conventional press forming, the enormous forces involved in the process, and the dedicated tooling. Traditionally, SPIF processes use small size tools (under 10 mm radius), but probably to the particular geometry of the test, larger tool radius can be employed successfully, producing a combination of failure modes and strain distribution in between conventional press forming and SPIF.

## Conclusions and future works

A series of tests have been performed under SPIF conditions and conventional press forming to study the evolution of the strain distribution on the outer surface of the specimens and the location of the failure. The main conclusions can be summarised as follows:

- The *LFR* was higher in single-stage SPIF with a 20 mm tool radius than the one using a 10 mm tool radius and the conventional forming with a 47.9 mm punch radius. This suggests that a threshold tool radius must exist that maximises the *LFR* in the flanging process.
- The same failure mechanism (onset of necking and subsequent fracture) and the same location (flange edge) were found in both hole flanging operations by single-stage SPIF with a 20 mm tool radius and conventional flanging. Besides, the strain distributions of both processes have the same shape in the FLD.
- Nevertheless, the incremental effect of the SPIF process is clearly appreciated in the FLD by strains well above the FLC for necking. This indicates that the conventional FLC is not applicable for SPIF even if the failure mechanism is necking.

Next steps to complete this study are currently in progress:

- Development of a numerical model to accurately predict the stress and strain distribution during the flanging process.
- Analysis of formability limits and failure mechanism in the average stress triaxiality versus the equivalent plastic strain space in order to elucidate the transition from incremental to conventional forming of hole-flanged parts.
-

## Acknowledgements

The authors acknowledge the funding provided by Grant PID2021-125934OB-I00 financed by MCIN/AEI/10.13039/501100011033 and by ERDF 'A way of making Europe' (EU).

## References

[1] Emmens, WC, van den Boogaard, AH., An overview of stabilizing deformation mechanisms in incremental sheet forming. Journal of Materials Processing Technology 209 (2009)3688– 3695. https://doi.org/10.1016/j.jmatprotec.2008.10.003

[2] Silva MB, Skjoedt M, Atkins AG, Bay N, Martins PAF Single point incremental forming & formability/failure diagrams. J Strain Anal Eng Des 43 (2008) 15–36. https://doi.org/10.1243/03093247JSA340

[3] Silva, MB., Nielsen, PS., Bay, N., Martins, PAF., Failure mechanisms in single point incremental forming of metals. International Journal of Advanced Manufacturing Technology 56 (2011) 893-903. https://doi.org/10.1007/s00170-011-3254-1

[4] Martínez-Donaire, A.J., Borrego, M., Morales-Palma, D., Centeno, G., Vallellano, C.: Analysis of the influence of stress triaxiality on formability of hole-flanging by single-stage SPIF. Int. J. Mech. Sci. 151, 76–84 (2019). https://doi.org/10.1016/j.ijmecsci.2018.11.006

[5] Mosecker, L., Gottmann, A., Saeed-Akbari, A., Bleck, W., Bambach, M., Hirt, G., Deformation mechanisms of Ti6Al4V sheet material during the incremental sheet forming with laser heating. Key Eng. Mater. 549 (2013) 372–380. https://doi.org/10.4028/www.scientific.net/KEM.549.372

[6] Chang, Z., Yang, M., Chen, J., 2. Experimental investigations on deformation characteristics in microstructure level during incremental forming of AA5052 sheet. J. Mater. Process. Technol. 291 (2001) 117006

[7] Huang, Y.M., Chien, K.H. Influence of the punch profile on the limitation of formability in the hole-flanging process. Journal of Materials Processing Technology 113 (2001) 720-724. https://doi.org/10.1016/S0924-0136(01)00597-0

[8] Huang, Y.M., Chien, K.H. The formability limitation of the hole-flanging process. Journal of Materials Processing Technology 117 (2001) 43-51. https://doi.org/10.1016/S0924-0136(01)01060-3

[9] Borrego, M., Morales-Palma, D., Martinez-Donaire, A.J., Centeno, G., Vallellano, C., Experimental study of hole-flanging by single-stage incremental sheet forming. Journal of Materials Processing Technology 237 (2016) pp. 320-330. https://doi.org/10.1016/j.jmatprotec.2016.06.026

[10] Martinez-Donaire, A.J., Garcia-Lomas, F.J., Vallellano, C., New approaches to detect the onset of localised necking in sheets under through thickness strain gradients. Materials and Design 57 (2014) 135–145. https://doi.org/10.1016/j.matdes.2014.01.012

[11] Cristino, V.,Silva, M. B., Wong, P., Martins, P.A.F. Determining the fracture forming limits in sheet metal forming: A technical note. The Journal of Strain Analysis for Engineering Design. 52 (2017). https://doi.org/10.1177/0309324717727443

[12] Borrego, M., Morales-Palma, D., Martínez-Donaire, A.J., Centeno, G., Vallellano, C., Analysis of formability in conventional hole flanging of AA7075-O sheets: punch edge radius effect and limitations of the FLC. Int J Mater Form 13, 303–316 (2020). https://doi.org/10.1007/s12289-019-01487-2